Local Valleys Cause Deviations in Latitudinal Warming Trends in Italy

Linda L. Chen

January 12, 2020

Abstract

As Earth's average temperature rises, Italy is one of several regions on Earth experiencing the most severe warming. This research investigates how local geography affect the rate at which local Italian regions are warming. Using weather model data of over 30 regions, I found the rate at which each region is warming and compared each rate to different latitude and ruggedness of a region. To quantify ruggedness, I gathered topographic data corresponding each weather model region and created an algorithm that calculates the valley index, which is the percentage of the area identified as a valley relative to the whole region. I found that Italian regions in higher latitudes warm faster for most terrains ($R^2 = 0.92$ and $p \leq 0.05$). However, regions with extreme valley indices (high and low) deviate from the latitudinal warming trend (warming slower and faster, respectively).

Key Points:

1. A new image processing algorithm that finds the local minimum is useful to find the percentage of valley areas per given region.
2. Regions in higher latitudes generally warm faster, but anomalies to this trend are planar and mountainous regions, which warm faster and slower respectively.

1 Introduction

As established by the report by Intergovernmental Panel on Climate Change (2014), anthropogenic forces such as carbon emissions have accelerated warming on a global scale in the past century.

On a regional scale, many areas show an increased warming; among them, Italy has increased by 1 °C in the past century. (Amendola et al., 2018; Brunetti et al., 2006). For reference, the entire Earth has warmed by 0.8 °C since 1885 (Hansen et al., 2010).

Researchers have found that the extreme warming in the Mediterranean Basin threatens a variety of domains, especially water scarcity, ecosystems, and agriculture (Cramer et al., 2018).

While there are studies about how anthropogenic (greenhouse gases and sulfate aerosols) forces cause plausible warming within the Mediterranean region (Barkhordarian et al., 2011), a better understanding of the climate trends in relation to geography is necessary to anticipate the negative impacts of climate change mentioned by Cramer et al. (2018). In addition, data from Amendola et al. (2018); Brunetti et al. (2006); Lobell et al. (2011) show data on grids at least 0.5° by 0.5° large in the geographic coordinate system. I investigate some factors such as latitude and distance from the ocean. In addition, Crouch (2015) claims that the mountains and valleys may affect the local climate of a region by altering how much solar energy is exposed to the region. To see the effect of terrain on the regions' warming, I developed an algorithm that estimates the ruggedness of a terrain by calculating the percentage of pixels that are part of a valley within a region. I then compare the percentage to the rate at which the region is warming.

2 Data and Methods

This study investigates 30 regions across Italy. Each region covers a 20 by 20 kilometer area (**Table 1**). The weather data is from Meteoblue[1]. Meteoblue uses multi-scale climate models that uses data from nearby weather stations and simulations. There are data for each hour from January 1st, 1985 to December 30th, 2018. As shown in **Figure 1**, I took the annual average of the temperature data in each region. I subtracted these yearly averages from the total average temperature of that region to obtain the anomalies for each year. Then I fitted a trend line of each time series, computing the overall change in temperature over 34 years by taking the difference in temperature at the ends of the line. I scaled the warming rate to a decade by multiplying by 10 and dividing by 34.

The elevation data is from Tarquini et al. (2007, 2012), who created a digital elevation model (DEM) of Italy called TINITALY/01. TINITALY/01 combines contour lines and spot heights de-

[1]Meteoblue is a meteorological service created at the University of Basel, Switzerland, in cooperation with the U.S. National Oceanic and Atmospheric Administration and the National Centers for Environmental Prediction. (**URL:** `https://content.meteoblue.com/en/about-us`)

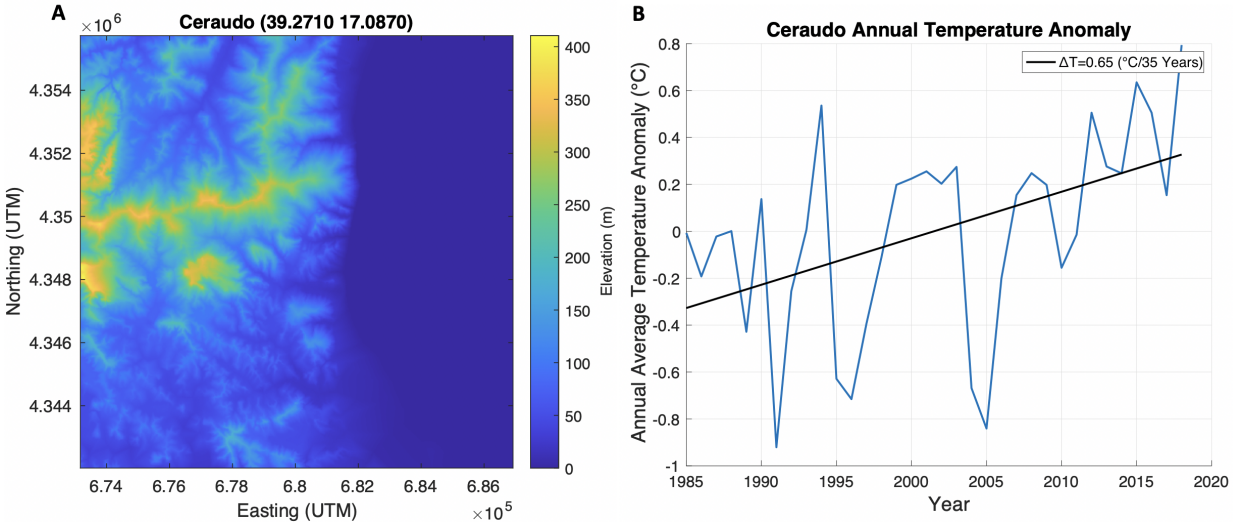

Figure 1: (A) Digital elevation model (DEM) of Tarquini et al. (2007, 2012) Ceraudo, Italy, one of the cites sampled using the Meteoblue data. Ceraudo is a costal region located in southern Italy. (B) A graph of the yearly average temperature data from 1985 to 2018 with a trend line fit to measure the warming rate of the region. Ceraudo is has increased by 0.65 °C from 1985 to 2018.

rived from the Italian Regional topographic maps, satellite-based global positioning system points, ground based and radar altimetry data. The resolution of these images are 10 by 10 meters. For the consistency of measurement, the 20 by 20 kilometer grid from TINITALY/01 is centered at the same coordinates used for the Meteoblue data.

The algorithm to compute the valley index initially converts the elevation data into a gray scale image (**Figure 2 B**), which is adapted from Robert (2015). I then filtered the image into a low (black) and high (white) elevation with a specific threshold (**Figure 2 C**). Since valleys appear at different elevations, the filter uses an adaptive threshold method developed by Bradley & Roth (2007) (**Figure 2 C**). The filter computes the threshold at a pixel by finding the local mean intensity around the neighborhood of the pixel. The neighborhood size of the image is computed as:

$$\psi \quad = \quad 2 * floor(\frac{\phi}{16} + 1) \tag{1}$$

where ϕ is the size of the image in pixels and ψ is the size of the neighborhood in pixels. The neighborhood is roughly $1/8$th the size of the image. Since every region has a different terrain, each threshold value is different for each region. Through visual inspection, I recorded which threshold values best captured the valley in a region. I correlated the threshold values to different topographic regions (maximum height, minimum height, range) and found a strong correlation between range of elevation and the threshold values (see **Figure 6 in Section 7**). This equation thus calculates the threshold value as:

$$\tau = -0.108 * \ln \epsilon + 1.384 \tag{2}$$

where τ is the threshold and ϵ is the difference between the maximum and minimum elevation of a region. However, certain areas have flat areas (ocean, lake, planes) that are included in the valley region. To remove this area, a histogram of the elevation data is computed with each elevation as a percentage of the entire region. The number of specific elevation section is determined by:

$$\nu = 1.5 * round(\log_2(\chi) + 1) \tag{3}$$

Where ν is the number of bins in the histogram and χ the product of all the values in the sample. A flat area is when the bottom section of the elevation is more than 10 percent of the region. (**Figure 2 E**) If there is a flat area, a filter removes the flat ground from whatever region calculated through adaptive thresholding.(**Figure 2 E and G**). Then I divided the area of the valleys (**Figure 2 H**) from the total area of the region to find the valley index. I then correlated the warming rate with different geographic factors (latitude, distance from the ocean, elevation, valley index).

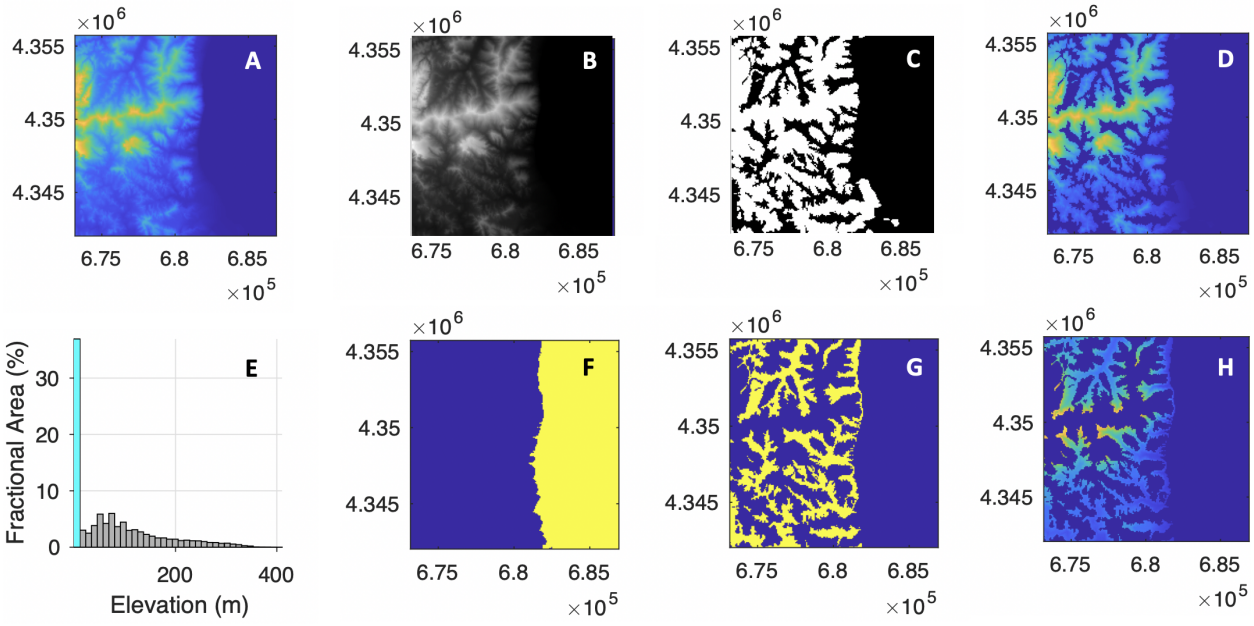

Figure 2: Algorithm used to compute the percentage of valleys at a Ceraudo (coordinates in UTM). With the topography data (A), the algorithm converts the data into a gray scale image (B) uses the adaptive threshold (C) to identify the lower regions (D). In order to remove the ocean from the valley index, a histogram of the elevation data is calculated (see **Equation 3**). (E) Ceraudo has a flat ground percentage of 36.93 percent of an elevation of about 5.7 m, so a flat ground filter was applied (F) and subtracted from the original filtered area (G to H). The calculated valley index for Ceraudo is 22 percent.

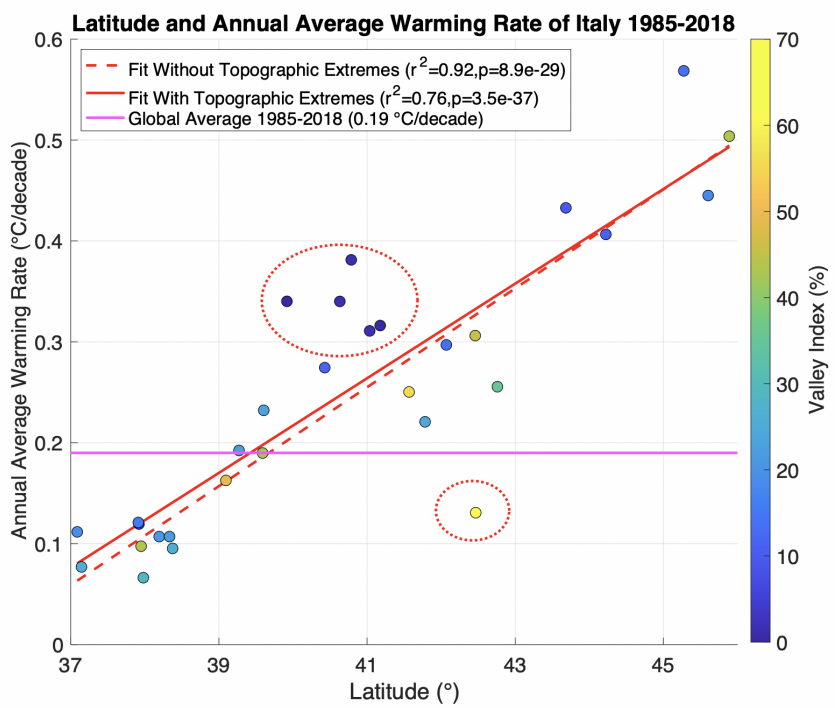

Figure 3: Warming rate, in °C per decade, of all 30 locations with respect to latitude. Without the anomalies (circled in red), $R^2 = 0.92$ and $p = 8.9 * 10^{-29}$. In addition, Italy is warming at a faster rate than the global rate from 1985-218 from (Smith et al., 2008). The valley index shows how the five points clustered together have a very low valley index and the single yellow point has a high valley index. The pink is the global temperature anomaly from Smith et al. (2008), which is under the majority of regions derived from the Meteoblue data.

3 Results

After computing the change in temperature of the region from the anomalies, I found that all of the locations are warming ranging from 0.0663 to 0.5685 °C per decade. Of the four geographic variables, latitude formed the strongest pattern correlation with the warming rate of the locations. However, there are two groups of anomalies identified in the graph (**Figure 3**) that have extreme values of the valley index. The region with the lower warming rate (yellow in **Figure 3**) is Terminillo Mountain (**Figure 4 B**). The region with a higher warming rate from regions in the 39 to 42 ° latitude (indigo in **Figure 3**) are identified as the flattest regions (**Figure 4 C**). In (**Figure 6**), these regions are all from the Apulia region, which is one of the flattest regions in Italy. Without the anomalies the linear fit linear has an R^2 value of 0.92 and a p of $8.9 * 10^{-29}$.

4 Discussion

The correlation between latitude and warming rate brings attention to the impact of varying rates in each region. While latitude is correlated with the warming rate of each location, the other factors related to latitude should be examined. For example, areas in higher latitudes experience less sunlight exposure due to the Earth's tilt.

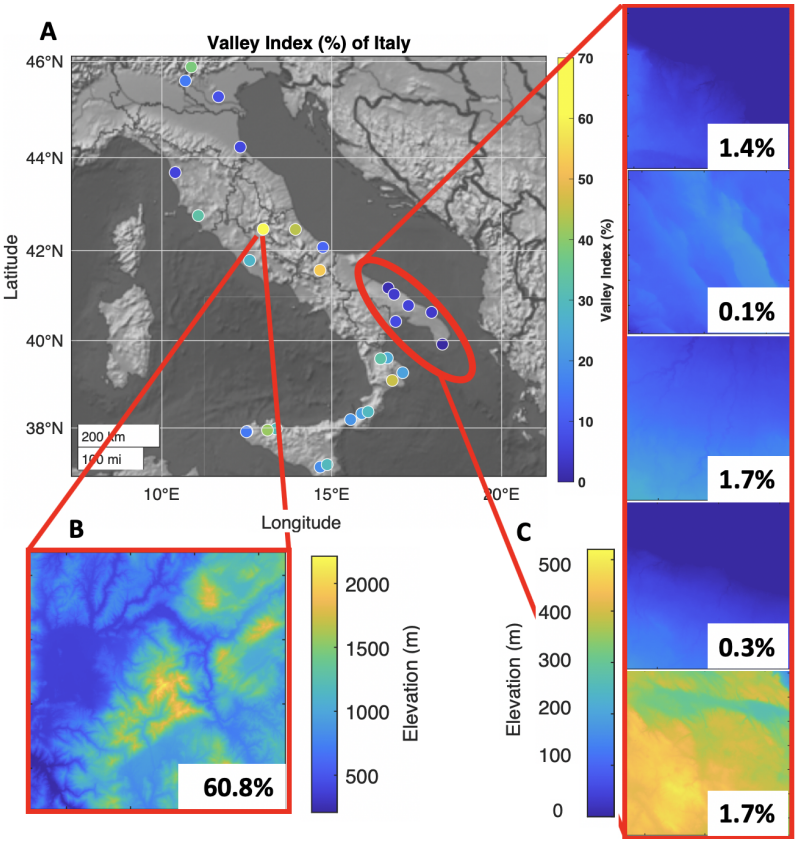

Figure 4: (A) Regions identified as anomalies in (**Figure 4**). The high valley index is Terminillo Mountain, which has a valley index of 60.8 percent (B) and is located in the Abruzzi Apennine region of Italy. Meanwhile the regions with the higher warming rate than those in similar latitudes with a low valley index (C) are all located in the Apulia Region (from top to bottom: Brindisi, Darioratta, Frantoio De Carlo, Olio Intini, and Tre Colonne) where the terrain is relatively flatter than the rest of Italy.

Data from Smith et al. (2008) on a 5° by 5° grid confirms the general pattern and magnitude of warming (0.3 to 0.4 °C per decade) of Apulia Region warming faster than those in its region. However, the absolute value derived form Meteoblue is more variable and specific (highlighting the anomaly of Terminillo Mountain). In addition, most of the regions in Italy are warming faster than the global average derived from Smith et al. (2008) (0.19 °C per decade) (**Figure 3**), confirming the general conclusions of Amendola et al. (2018); Brunetti et al. (2006); Lobell et al. (2011).

The step in the valley index algorithm that computes the percentile of flat area and subtracts the valley image from that flat ground only looks at the lowest section of data (**Figure 2 E**). This step does not take into account flat areas that may be in elevations higher than the bottom section, such as lakes on mountains or plateaus. While the algorithm needs to be modified, it would be interesting to see how the topography of those regions may affect the regions' warming rate.

Aside from topography, other variables-such as humidity, temperature of the bodies of water-should be tested to create a more accurate model of the warming of regions in Italy. To refine the experiment even further, more locations should be sampled. However, Hereher (2016) found that along with latitude and topography, the composition of the ground and surface albedo (surface reflection of solar radiation) may cause different regions to warm faster than others.

Here we examined general trends in global warming in small, specific regions. It would be interesting to see if these trends are specific to Italy or can be applied to other regions across the world.

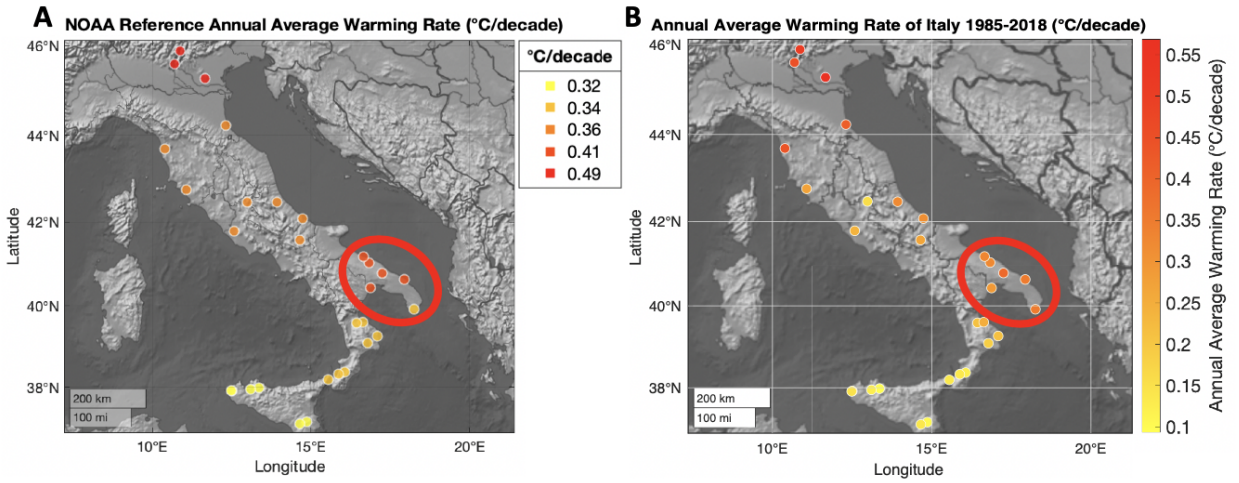

Figure 5: (A) Data extracted from Smith et al. (2008), which consists of monthly average temperature anomalies on a 5 ° by 5 ° grid across land and ocean surfaces. Compared to the Smith et al. (2008) global average in **Figure 3** (0.19 °C per decade), all of Italy is warming faster. However, the rates calculated by Meteoblue are higher than both averages calculated by Smith et al. (2008). Yet the general trend of the Apulia Region (B, circled in red) warming faster than everywhere except northern Italy is reflected in both (A) and (B).

5 Conclusions

Here I show that both model data derived from simulations and recorded data from Meteoblue and Smith et al. (2008) show how local regions in Italy generally follow a warming pattern based on latitude. I created a rudimentary algorithm that calculates the percentage of valley area relative to each region in Italy using an adaptive threshold method in image processing. Regions with extreme valley indices have shown to deviate from the linear pattern with latitude and warming rate. These findings show how we need to investigate how the warming rate in these regions on a local level to prepare for the challenges of global warming.

6 Acknowledgements

Thank you Frederik Simons for providing most of the data analysis code, as well as extract 10 more regions from TINITALY/01 and helping me organize the data. Thank you to Adam Maloof, who provided endless guidance and direction, as well as obtaining the Meteoblue weather data.

Thank you Franklyn Correa and Lauren Blackburn for explaining the correlation matrices. Stacey Edmonsond, Bolton Howes, and Alex Cox helped with debugging the code, providing feedback, and guidance for my research. I am grateful for Melvin Bulacia, who provided valuable feedback for my paper. I also thank the staff at the Princeton Writing Center for helping with the clarity and accessibility of my paper.

References

Amendola, S., Maimone, F., Pelino, V. & Pasini, A., 2018. New records of monthly temperature extremes as a signal of climate change in italy, *International Journal of Climatology*, **39**(4), 2491–2503. doi: 10.1002/joc.5952.

Barkhordarian, A., Bhend, J. & von Storch, H., 2011. Consistency of observed near surface temperature trends with climate change projections over the mediterranean region, *Climate Dynamics*, **38**(9-10), 1695–1702. doi: 10.1007/s00382-011-1060-y.

Bradley, D. & Roth, G., 2007. Adaptive thresholding using the integral image, *Journal of Graphics Tools*, **12**(2), 13–21, Obtained from https://www.mathworks.com/help/images/ref/imbinarize.html as the function imbinarize.

Brunetti, M., Maugeri, M., Monti, F. & Nanni, T., 2006. Temperature and precipitation variability in italy in the last two centuries from homogenised instrumental time series, *International Journal of Climatology*, **26**(3), 345–381. doi: 10.1002/joc.1251.

Cramer, W., Guiot, J., Fader, M., Garrabou, J., Gattuso, J.-P., Iglesias, A., Lange, M. A., Lionello, P., Llasat, M. C., Paz, S., Penuelas, J., Snoussi, M., Toreti, A., Tsimplis, M. N. & Xoplaki, E., 2018. Climate change and interconnected risks to sustainable development in the mediterranean, *Nature Climate Change*, **8**, 972–980.

Crouch, J., 2015. The Highs and Lows of Climate, *Climate.gov*.

Hansen, J., Ruedy, R., Sato, M. & Lo, K., 2010. GLOBAL SURFACE TEMPERATURE CHANGE, *Reviews of Geophysics*, **48**(4). doi: 10.1029/2010rg000345.

Hereher, M. E., 2016. Time series trends of land surface temperatures in egypt: a signal for global warming, *Environmental Earth Sciences*, **75**(17). doi: 10.1007/s12665-016-6024-4.

Intergovernmental Panel on Climate Change, 2014. *Climate Change 2013: The Physical Science Basis*, Cambridge University Press.

Lobell, D. B., Schlenker, W. & Costa-Roberts, J., 2011. Climate trends and global crop production since 1980, *Science*, **333**(6042), 616–620. doi: 10.1126/science.1204531.

Robert, N., 2015, *Automatic Detection of Vally Forms*, mathesis, University of Oslo.

Smith, T. M., Reynolds, R. W., Peterson, T. C. & Lawrimore, J., 2008. Improvements to NOAA's historical merged land–ocean surface temperature analysis (1880–2006), *Journal of Climate*, **21**(10), 2283–2296.

doi: 10.1175/2007jcli2100.1.

Tarquini, S., Isola, I., Favalli, M., Mazzarini, F., Bisson, M., Pareschi, M. T. & Boschi, E., 2007. TINITALY/01: a new triangular irregular network of Italy, *Ann. Geophys.*, **50**(3), 407–425, doi: 10.4401/ag–4424.

Tarquini, S., Vinci, S., Favallia, M., Doumaz, F., Fornaciai, A. & Nannipieri, L., 2012. Release of a 10-m-resolution DEM for the Italian territory: Comparison with global-coverage DEMs and anaglyph-mode exploration via the web, **38**(1), 168–170, doi: 10.1016/j.cageo.2011.04.018.

7 Appendix

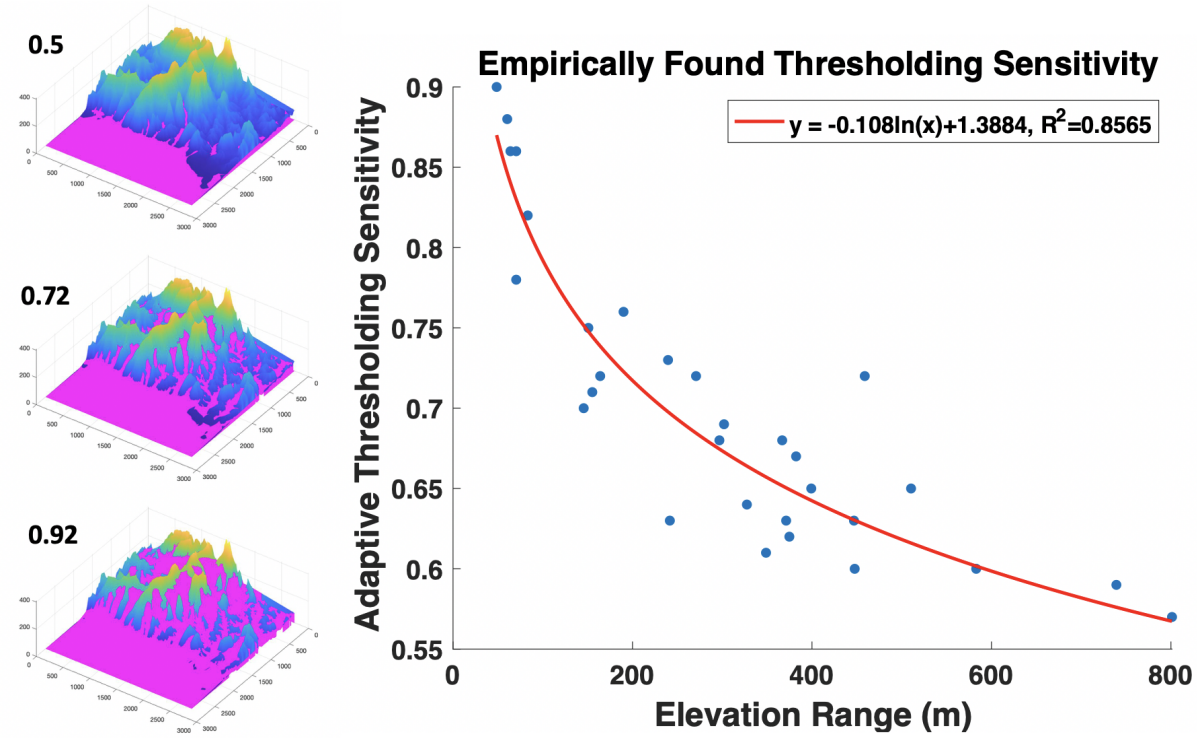

Figure 6: Empirically derived adaptation threshold. On the left there is the digial elevation model (DEM) and the region identified by the filter using different thresholds. The top one is too small, bottom too much, and middle accurately identifying the valleys. On the right is the recorded thresholds with respect to the regions elevation range. With an $R^2 = 0.8565$, there is a significant correaltion in which the equation describing the seried can be used to calculate the threshold from the DEM.

Location Name	Lat.	Lon.	$Elev_{MAX}$ (m)	$Elev_{MIN}$ (m)	Range (m)	Avg. Gradient	Exp Threshold	Calc Threshold	mb Rise (°C/34 yrs)	NOAA Rise (°C/10 yrs)
Agrestis	37.144	14.864	986	167.75	818.25	0.74	0.64	0.260	0.262	0.32
Baglio di Pianetto	37.979	13.362	1085	148	937	0.9	0.62	0.288	0.225	0.32
Brindisi	40.632	17.936	121.48	0	121.48	0.07	0.9	0.015	1.156	0.41
Campobasso	41.567	14.650	1921	1760	161	1.13	0.86	0.560	0.851	0.36
Ca' Rainene	45.605	10.693	1184	65	1119	0.9	0.6	0.181	1.513	0.49
Ceraudo	39.271	17.087	410	0	410	0.48	0.72	0.223	0.654	0.34
Cervia	44.224	12.307	475	0	475	0.2	0.76	0.111	1.382	0.36
Dario Ratta	39.918	18.255	188.92	12.16	176.76	0.11	0.78	0.001	1.157	0.34
Enotre	39.094	16.779	1532	74.54	1457.46	0.91	0.6	0.492	0.553	0.34
Feudo Disisa	37.949	13.108	1068	140	928	0.54	0.63	0.438	0.332	0.32
Frantoi Cutera	37.087	14.659	905.59	163.48	742.11	0.46	0.68	0.190	0.380	0.32
Frantoio Acri	39.605	16.633	998	0	998	0.62	0.65	0.236	0.789	0.34
Frantoio De Carlo'	41.035	16.833	231	23	208	0.08	0.82	0.017	1.057	0.41
Frantoio di Cornoleda	45.276	11.666	600	0.48	599.52	0.41	0.73	0.134	1.933	0.49
Frantoio Hermes	42.460	13.930	1213	67	1146	0.61	0.72	0.456	1.041	0.36
Grosseto	42.760	11.072	631	-46.11	677.11	0.52	0.72	0.353	0.869	0.36
Laselvotta	42.070	14.739	364	0	364	0.33	0.7	0.138	1.010	0.36
Marina di Ginosa	40.428	16.880	388	0	388	0.26	0.71	0.120	0.933	0.41
Messina	38.194	15.553	1276	0	1276	1.51	0.65	0.215	0.364	0.34
Olearia San Giorgio	38.375	16.067	964	91.27	872.73	0.56	0.61	0.257	0.324	0.34
Olio Cru	45.890	10.866	2013	65	1948	2.05	0.59	0.437	1.713	0.49
Olio Intini	40.786	17.254	502	129.91	372.09	0.2	0.75	0.017	1.296	0.41
Pisa	43.684	10.393	914	-2.96	916.96	0.4	0.68	0.100	1.471	0.36
Roma Ciampino	41.783	12.583	955.7	0	955.7	0.32	0.67	0.248	0.751	0.36
Sorelle Garzo	38.333	15.882	604	0	604	0.61	0.63	0.218	0.364	0.34
Tenute Librandi Pasquale	39.590	16.436	1123	6	1117	0.66	0.63	0.429	0.645	0.34
Titone	37.920	12.508	151	0	151	0.1	0.88	0.042	0.406	0.32
Terminillo Mountain	42.467	12.983	2212	209	2003	1.83	0.57	0.609	0.444	0.36
Trapani-Birgi	37.911	12.488	755	0	755	0.4	0.69	0.154	0.411	0.32
Tre Colonne	41.177	16.658	176	0	176	0.08	0.86	0.003	1.075	0.41

Table 1: Table of all the locations sampled in the area from 1985 to 2018. The NOAA data is obtained from Smith et al. (2008).